

PAPER • OPEN ACCESS

Peristaltic motion of a Bingham fluid in contact with a Newtonian fluid in a vertical channel

To cite this article: J Suresh Goud *et al* 2017 *IOP Conf. Ser.: Mater. Sci. Eng.* **263** 062005

View the [article online](#) for updates and enhancements.

Related content

- [An Analysis of Peristaltic Flow of a Micropolar Fluid in a Curved Channel](#)
N. Ali, M. Sajid, T. Javed *et al.*
- [Microconvection in vertical channel at given heat flux](#)
V B Bekezhanova and I A Shefer
- [Rayleigh–Taylor instability in a viscoplastic fluid](#)
A Yu Demianov, A N Doludenko, N A Inogamov *et al.*



ECS **240th ECS Meeting**
Oct 10-14, 2021, Orlando, Florida

Register early and save up to 20% on registration costs

Early registration deadline Sep 13

REGISTER NOW

Peristaltic motion of a Bingham fluid in contact with a Newtonian fluid in a vertical channel

J Suresh Goud¹, R Hemadri Reddy¹, and R Saravana²

¹Department of Mathematics, School of Advanced Science, VIT University, Vellore 632014, India

²Department of Mathematics, Madanapalle Institute of Technology and Science, Madanapalle 517 325, India

E-mail: rhreddy@vit.ac.in

Abstract: Peristaltic motion of a Bingham fluid in contact with a Newtonian fluid in a Vertical channel has been studied under long wavelength and low Reynolds number suspensions. The flow is investigated in a wave frame of reference moving with velocity of the wave. The solution is acquired for stream function, velocity field, friction force and the pressure rise in several sectors over one cycle of wavelength. The impacts of yield stress on the frame of interface are contemplated. It is discovered that the time-averaged flux against pressure rise is decreasing with an increase in the yield stress and viscosity ratio and it is also identified that the frictional force has unsimilar behavior with pressure rise

1. Introduction

The conversation peristalsis stems from the Grecian word peristalikos, which means fastening and compacting. It is utilized to describe a progressive wave of recession along a channel or tube whose cross-sectional range subsequently differs. In physiology, it has been observed to be engaged with numerous natural organs. Specifically, peristalsis might be a fundamental system for pee transport from kidney to bladder through the ureter, development of chyme in the gastrointestinal tract, transport of lymph in the lymphatic vessels and the vasomotion of little veins. In addition, peristaltic pumps are composed by engineers for directing destructive fluids without contact with the walls of the pumping apparatus. Applying a wave frame of reference, Jaffrin and Shapiro [1] made a point by point investigation on the peristaltic pumping of a viscous fluid under long wave length and low Reynolds number suppositions.

It is distinguished in some physiological frameworks, such as throat and ureter that the wall of the structure doing the pumping is normally covered with a fluid with various properties from those of the fluid being pumped. In order to have an understanding about the result of fluid covering on the motion, the single fluid analysis of peristaltic pumping is extended to two fluid analysis by including peripheral layer of distinct viscosity. This investigation was first done by Shukla et al. [2] for channel and axisymmetric geometries. For non-uniform axisymmetric tubes, Srivastava and Srivastava [3] made an important contribution in peristaltic pumping. Brasseur et al. [4] made a significant contribution on the peristaltic motion of two immiscible fluids in a channel using flexible walls and have demonstrated the deficiency of the examination specified above in the limit of vast peripheral layer thickness. This problem is solved for axisymmetric case by Ramachandra Rao and Usha et al.



[5]. Usha and Ramachandra Rao [6] discussed the peristaltic pumping of two layered power-law fluids in an axisymmetric tube. The interface between the two layers is resolved from a transcendental equation in the centre radius. All these authors have specified the interface shape. Comparani and Mannucci [7] analyzed the flow of a Bingham fluid in contact with a Newtonian fluid in a channel. Vajravelu et al. [8] studied Peristaltic pumping of a Herschel-Bulkley fluid in contact with a Newtonian fluid. Vajravelu et al. [9] discussed Peristaltic transport of a Casson fluid in contact with a Newtonian fluid in a circular tube with permeable wall. The authors Narahari and Sreenadh [10], Kumar et al. [11] and Hari Prabhakaran et al. [12] studied the peristaltic pumping of a Bingham fluid in contact with a Newtonian fluid under the long wavelength approximation. Sreenadh et al. [13] discussed the peristaltic motion of a power law fluid in contact with a Jeffrey fluid in an inclined channel with permeable walls. Kavitha et al. [14] studied peristaltic transport of a Jeffrey fluid in contact with a Newtonian fluid in an inclined channel.

Motivated by these facts, we propose to talk the peristaltic motion of a Bingham fluid in contact with a Newtonian fluid in vertical channel. This ideal may be helpful to comprehend the peristaltic motion of blood in vertical small vessels. The velocity field, the stream function, the friction force and the pressure rise over one cycle of wavelength are acquired.

2. Mathematical development

Consider the peristaltic motion of a bio-fluid consisting of two immiscible and incompressible fluids of distinct viscosities μ_1 and μ_2 holding the core by a Bingham fluid and peripheral layer by a Newtonian fluid in a channel with half-width a .

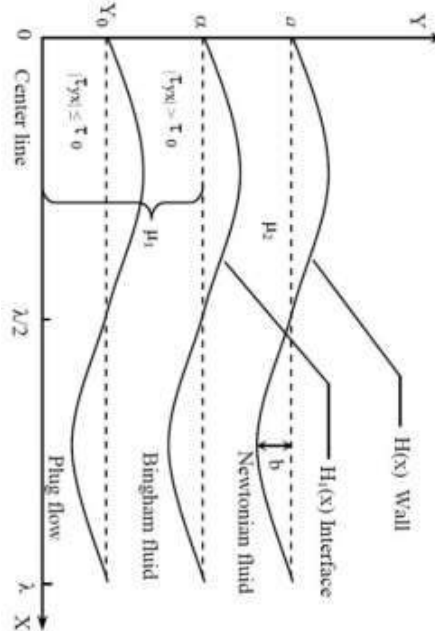


Figure 1. Schematic diagram of the physical pattern

The wall deformation due to the proliferation of an immense train of peristaltic waves is given by

$$Y = H(X, t) = a + b \cos \frac{2\pi}{\lambda} (X - ct) \quad (1)$$

where b is the amplitude, λ is the wavelength and c is the wave speed. The resulting distortion of the interface isolating the core and peripheral layer is denoted by $Y = H_1(X, t)$ (figure 1) which is not known from the earlier.

2.1 descriptions of Motion

Under the suspicions that length of the channel is an essential numerous of the wavelength, the pressure difference over the wavelength is steady and the periodicity of the interface is same as that of

the peristaltic wave. The flow frame turns out to be consistent in the wave frame moving with velocity c away from the fixed frame (X, Y) called laboratory frame. The conversion between these two frames is given by

$$x = X - ct, y = Y, u(x, y) = U(X - ct, Y) - c, v(x, y) = V(X - ct, Y), p(x) = P(X, t), \psi = \Psi - Y \quad (2)$$

Where ψ and Ψ are the stream functions in the wave and laboratory frames respectively. Applying the non-dimensional quantities

$$\begin{aligned} \bar{x} = \frac{x}{\lambda}, \bar{y} = \frac{y}{a}, \bar{h} = \frac{h}{a}, \bar{h}_1 = \frac{h_1}{a}, \bar{t} = \frac{ct}{\lambda}, \bar{P} = \frac{Pa^2}{\mu_1 \lambda c}, \bar{\phi} = \frac{b}{a}, \bar{\tau}_0 = \frac{a\tau_0}{\mu_1 c}, \bar{y}_0 = \frac{y_0}{a}, \bar{q} = \frac{q}{ac}, \\ \bar{\psi}^{(i)} = \frac{\psi^{(i)}}{ac}, \bar{\eta} = \frac{\rho g a^2}{\mu_1 c}, \bar{F} = \frac{Fa}{\mu_1 \lambda c}, \bar{u}^{(i)} = \frac{u^{(i)} \lambda}{c} = -\frac{\partial \bar{\psi}^{(i)}}{\partial \bar{y}}, \bar{v}^{(i)} = \frac{v^{(i)} \lambda}{ac} = -\frac{\partial \bar{\psi}^{(i)}}{\partial \bar{x}} \quad (i=1,2), \\ \bar{\mu} = \begin{cases} 1, & 0 \leq \bar{y} \leq \bar{h}_1 \\ \mu \left(= \frac{\mu_2}{\mu_1} \right), & \bar{h}_1 \leq \bar{y} \leq \bar{h} \end{cases} \quad (3) \end{aligned}$$

where $\bar{v}^{(i)}$ and $\bar{u}^{(i)}$ are the \bar{y} and \bar{x} components of velocities in the wave frame ($i=1,2$) indicates core and peripheral layers respectively, p is the pressure,

The governing equations of the motion under the lubrication path (dropping the bars),

$$\frac{\partial}{\partial y} \left[-\tau_0 + \frac{\partial^2 \psi^{(1)}}{\partial y^2} \right] + \eta = \frac{\partial p}{\partial x} \quad (4)$$

$$0 = \frac{\partial p}{\partial y} \quad (5)$$

$$\frac{\partial^2}{\partial y^2} \left[\mu \frac{\partial^2 \psi^{(2)}}{\partial y^2} \right] = 0 \quad (6)$$

where τ_0 is the yield stress.

The dimensionless boundary conditions are

$$\psi^{(1)} = 0 \quad \text{at } y = 0 \quad (7)$$

$$\psi_{yy}^{(1)} = \tau_0 \quad \text{at } y = 0 \quad (8)$$

$$\psi^{(2)} = q = \text{constant} \quad \text{at } y = h \quad (9)$$

$$\psi^{(1)} = q_1 = \text{constant} \quad \text{at } y = h_1 \quad (10)$$

$$\psi_y^{(2)} = -1 \quad \text{at } y = h \quad (11)$$

Where q and q_1 are the aggregate and the centre fluxes respectively over any cross segment wave frame. Further the velocity and the shear stress are continuous over the interface. The peripheral layer flux is given by $q_2 = q - q_1$. It takes from the incompressibility of the fluids that q , q_1 and q_2 are

independent of x . The average non-dimensional volume flow rate \bar{Q} over one period $T \left(= \frac{\lambda}{c} \right)$ of the

peristaltic wave is characterized as

$$\bar{Q} = \frac{1}{T} \int_0^T \int_0^h (u+1) dy dt = \frac{1}{T} \int_0^T (q+h) dt = q + \frac{1}{T} \int_0^T h dt = q+1 \quad (12)$$

The stream function is obtained by applying the boundary conditions (7) to (11) to each other using the boundary conditions at the extremes of the channel given by indicating \bar{Q} or the pressure difference Δp crosswise over one wavelength

2.2 Solution

Solving equations (4) - (6) to each other using the boundary conditions (7) - (11) and

$$\psi^{(1)} = \psi_p^{(1)} \text{ at } y = y_0 \quad (13)$$

$$\psi_p^{(1)} = 0 \text{ at } y = 0 \quad (14)$$

where y_0 is the upper limit of the plug flow region and $\psi_p^{(1)}$ is the stream function in the plug flow region. We get the stream function in the core (plug flow region & non-plug flow region) and peripheral layer as

$$\psi_p^{(1)} = y \left[-1 - \tau_0(h_1 - y_0) + (F_2 - \mu y_0^2) \left[\frac{6(q+h) + 3\tau_0(h_1^2 - y_0^2)}{4(F_3 - \mu y_0^3)} \right] \right] \text{ for } 0 \leq y \leq y_0 \quad (15)$$

where $F_j = h^j + (\mu - 1)h_1^j$ ($j = 1, 2, 3$)

$$\psi^{(1)} = -y - \tau_0 h_1 y + \frac{\tau_0}{2} (y^2 + y_0^2) + \left(\frac{2(q+h) + \tau_0(h_1^2 - y_0^2)}{8(F_3 - \mu y_0^3)} \right) (6F_2 y - 2\mu(y^3 + 2y_0^3)) \text{ for } y_0 \leq y \leq h_1 \quad (16)$$

$$\psi^{(2)} = -y + (q+h) + \left(\frac{6(q+h) + 3\tau_0(h_1^2 - y_0^2)}{12(F_3 - \mu y_0^3)} \right) (3yh^2 - y^3 - 2h^3) \text{ for } h_1 \leq y \leq h \quad (17)$$

We obtained the axial pressure gradient from (4) or (6) as

$$\frac{dp}{dx} = - \left[\frac{6\mu(q+h) + 3\mu\tau_0(h_1^2 - y_0^2)}{2(F_3 - \mu y_0^3)} \right] + \eta \quad (18)$$

2.3 The description for the Interface

The streamline of interface is seen from the boundary condition (10). For a given algebra of the wave and the time averaged flux \bar{Q} , the distant interface $h_1(x)$ is solved from (13) with the boundary condition (10). Replace (10) in (13) we obtain the algebraic equation governing the interface $h_1(x)$ as

$$\tau_0 h_1^5 + 4(\mu - 1)h_1^4 - \left[2(q+h)(2\mu - 3) - 4q_1(\mu - 1) + \tau_0(3h^2 + y_0^2) \right] h_1^3 + \left[2\tau_0 h^3 h_1^2 \right] - \left[6qh^2 + 2h^3 + 4\mu y_0^3 - 3\tau_0 y_0^2 h^2 \right] h_1 + \left[4q_1 h^3 - 4q_1 \mu y_0^3 + 4(q+h)\mu y_0^3 - 2\tau_0 y_0^2 h^3 \right] = 0 \quad (19)$$

Where q_1 and q are independent of x . Applying the condition $h_1 = \alpha$, $y_0 = \beta$ at $x=0$ in equation (19), we obtain

$$q_1 = \frac{\left[\tau_0 \alpha^5 + 4(\mu - 1)\alpha^4 - \left[2(q+1)(2\mu - 3) + \tau_0(3 + \beta^2) \right] \alpha^3 + 2\tau_0 \alpha^2 \right] - \left[6q + 4\mu\beta^3 - 3\tau_0\beta^2 + 2 \right] \alpha + 4(q+1)\mu\beta^3 - 2\tau_0\beta^2}{4\mu\beta^3 - 4(\mu - 1)\alpha^3 - 4} \quad (20)$$

2.4 The Pumping Characteristics

Integrate the equation (18) about x over one wavelength we get the pressure rise (drop) over one cycle of the wave as

$$\Delta p = -3\mu q I_1 - 3\mu I_2 - \frac{3}{2} \mu \tau_0 I_3 + \eta \quad (21)$$

where $I_1 = \int_0^1 \frac{1}{h^3 - h_1^3 + \mu(h_1^3 - y_0^3)} dx$

$$I_2 = \int_0^1 \frac{h}{h^3 - h_1^3 + \mu(h_1^3 - y_0^3)} dx$$

$$I_3 = \int_0^1 \frac{h_1^2 - y_0^2}{h^3 - h_1^3 + \mu(h_1^3 - y_0^3)} dx$$

The dimensionless frictional force F at the wall crosswise over one wavelength is given by

$$F = \int_0^1 h \left(-\frac{dp}{dx} \right) dx = 3\mu q I_2 + 3\mu I_4 + \frac{3}{2} \mu \tau_0 I_5 - \eta I_6 \quad (22)$$

where

$$I_4 = \int_0^1 \frac{h^2}{h^3 - h_1^3 + \mu(h_1^3 - y_0^3)} dx$$

$$I_5 = \int_0^1 \frac{h(h_1^2 - y_0^2)}{h^3 - h_1^3 + \mu(h_1^3 - y_0^3)} dx$$

$$I_6 = \int_0^1 h dx$$

3. Results and Discussions

The frame of the interface for distinct yield stresses is displayed in Figure 2. We notice that the deviation of the interface frame for low yield stresses leads to a thinner peripheral-layer in the dilated region. The uniform sinusoidal interface frame is never acquired. The frame of the interface for distinct viscosity ratios is displayed in Figure 3. The deviation of the interface frame for low viscosity ratios leads to a thicker peripheral-layer in the dilated region. The uniform sinusoidal interface frame is never acquired.

The deviation of pressure rise with time averaged flux is determined from equation (21) for distinct values of yield stress τ_0 using $\alpha=0.7$, $\phi=0.6$, $\mu=0.1$, $\eta=1$ and is displayed in Figure 4. We notice that for a given flux \bar{Q} , the pressure difference Δp decreases with the increasing in τ_0 . For a given Δp , the flux depends on the yield stress and it decreases with increasing in τ_0 . The deviation of pressure rise with time averaged flux for distinct values of viscosity ratio μ using $\alpha=0.7$, $\phi=0.6$, $\tau_0=0.1$, $\eta=1$ and is displayed in Figure 5. We notice that for a given flux \bar{Q} , the pressure difference Δp decreases with the increasing in μ . For a given Δp , the flux depends on viscosity ratio and it decreases with increasing in μ . The deviation of pressure rise with time averaged flux for distinct values of gravity parameter η using $\alpha=0.7$, $\phi=0.6$, $\mu=0.1$, $\tau_0=0.1$ and is displayed in Figure 6. We notice that for a given flux \bar{Q} , the pressure difference Δp increases with the increasing in η . For a given Δp , the flux depends on the gravity parameter and it increases with increasing in η .

The Friction force with time averaged flux is determined from equation (22) for distinct values of yield stress τ_0 using $\alpha=0.7$, $\phi=0.6$, $\mu=0.1$, $\eta=1$ and is displayed in Figure 7. We notice that for a given flux \bar{Q} , the Friction force F increases with the increasing in τ_0 . For a given F , the flux depends on the yield stress and it increases with increasing in τ_0 . The Friction force with time averaged flux for distinct values of viscosity ratio μ using $\alpha=0.7$, $\phi=0.6$, $\tau_0=0.1$, $\eta=1$ and is displayed in Figure 8. We notice that for a given flux \bar{Q} , the Friction force increases with the increasing in μ . For a given F , the flux depends on viscosity ratio and it increases with increasing in μ . The Friction force with time averaged flux for distinct values of gravity parameter η using $\alpha=0.7$, $\phi=0.6$, $\mu=0.1$, $\tau_0=0.1$, and is displayed in Figure 9. We notice that for a given flux \bar{Q} , the Friction force decreases with the increasing in η . For a given F , the flux depends on the gravity parameter and it decreases with increasing in η . Also, the frictional force F has unsimilar behavior in comparison to pressure rise ΔP .

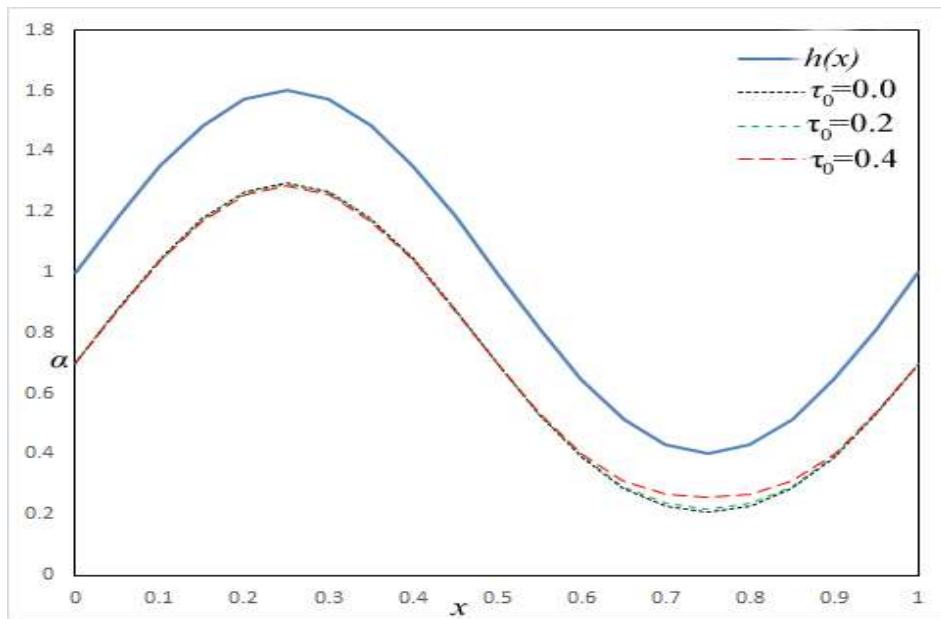


Figure 2. The frame of interface for distinct τ_0 using $\phi = 0.6, \mu = 0.9, \bar{Q} = 0.4, \alpha = 0.7$

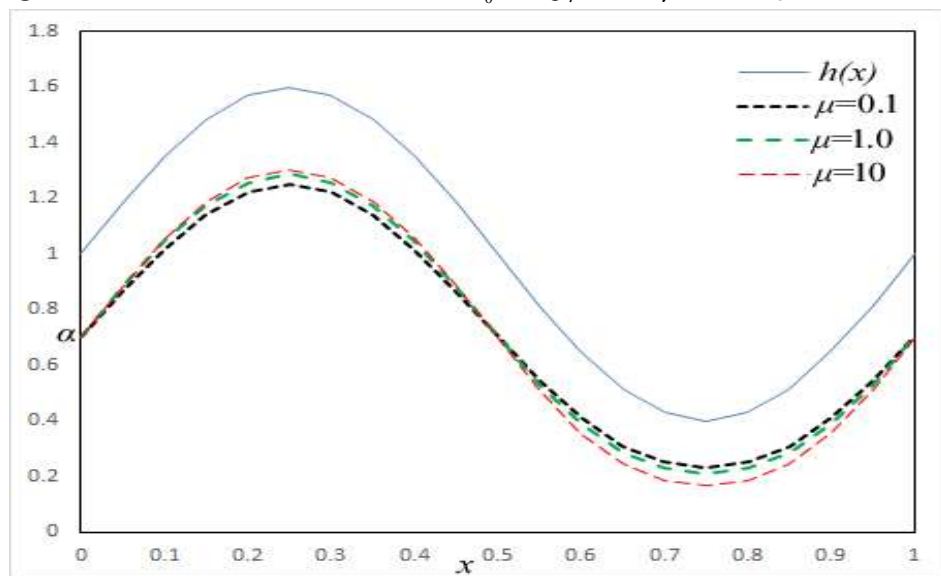


Figure 3. The frame of interface for distinct μ using $\phi = 0.6, \tau_0 = 0.1, \bar{Q} = 0.4, \alpha = 0.7$

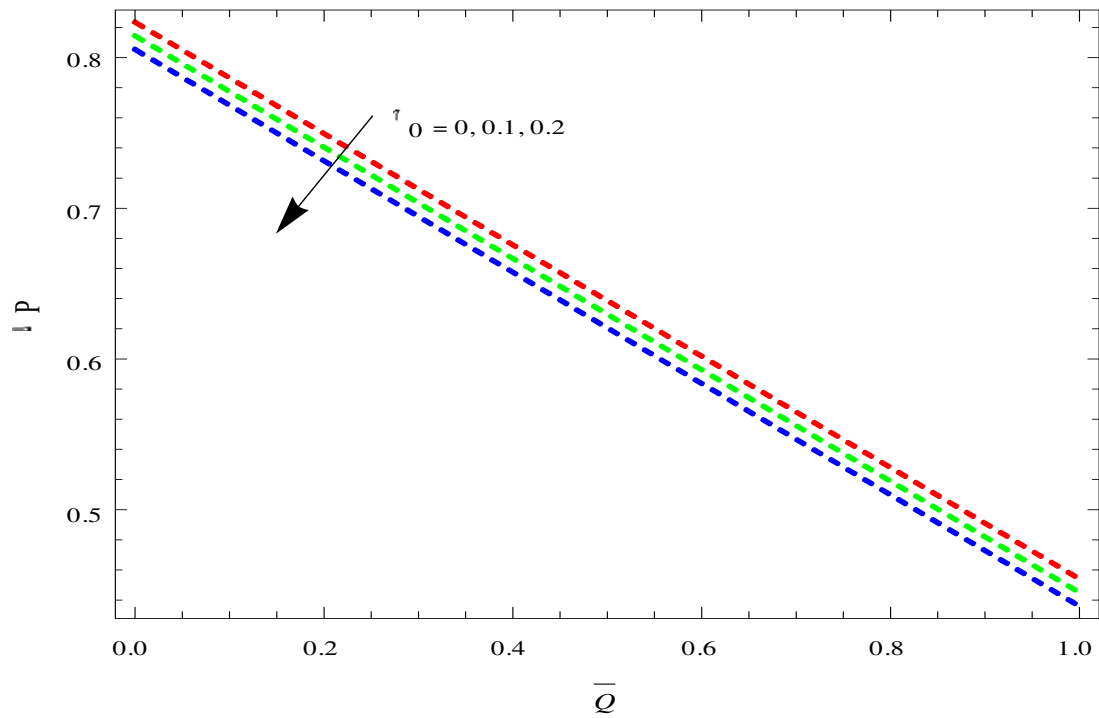


Figure 4. The deviation of Δp with \bar{Q} for distinct τ_0 using $\alpha = 0.7, \phi = 0.6, \mu = 0.1, \eta = 1$.

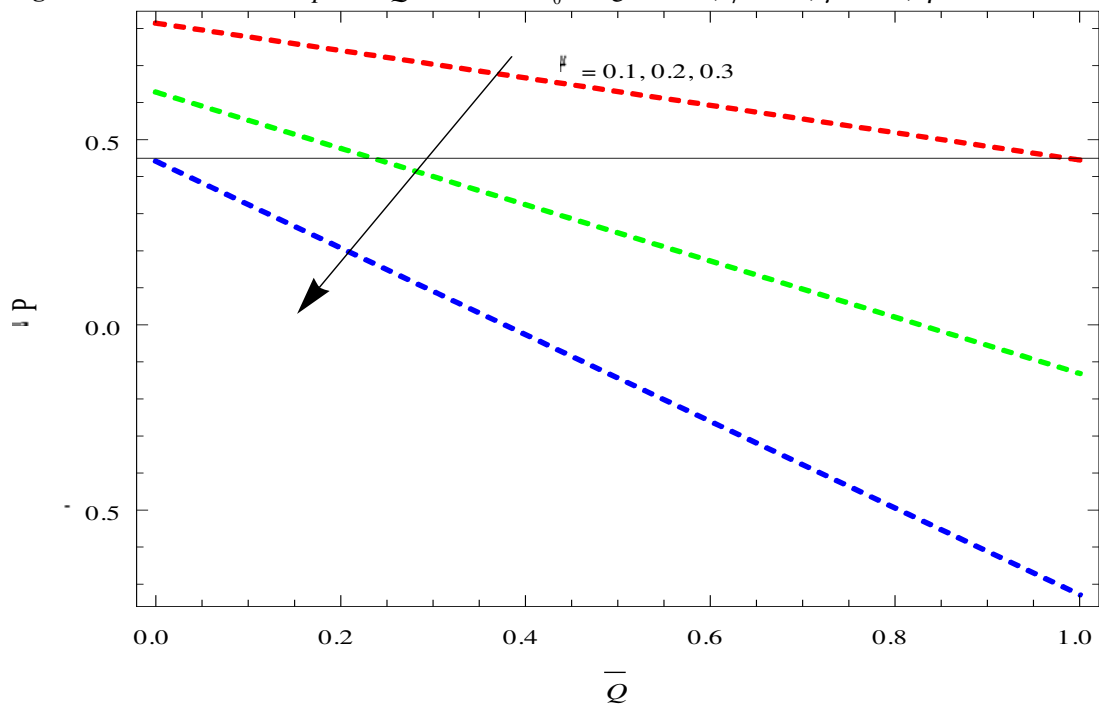


Figure 5. The deviation of Δp with \bar{Q} for distinct μ using $\alpha = 0.7, \phi = 0.6, \tau_0 = 0.1, \eta = 1$

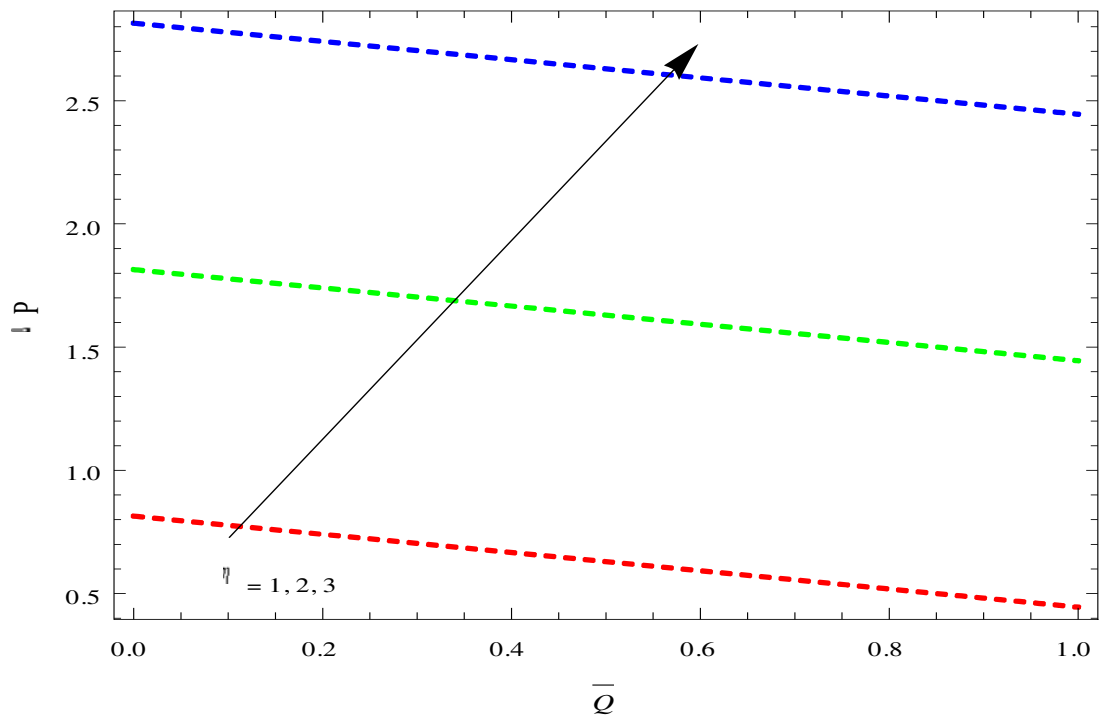


Figure 6. The deviation of Δp with \bar{Q} for distinct η using $\alpha = 0.7, \phi = 0.6, \mu = 0.1, \tau_0 = 0.1$.

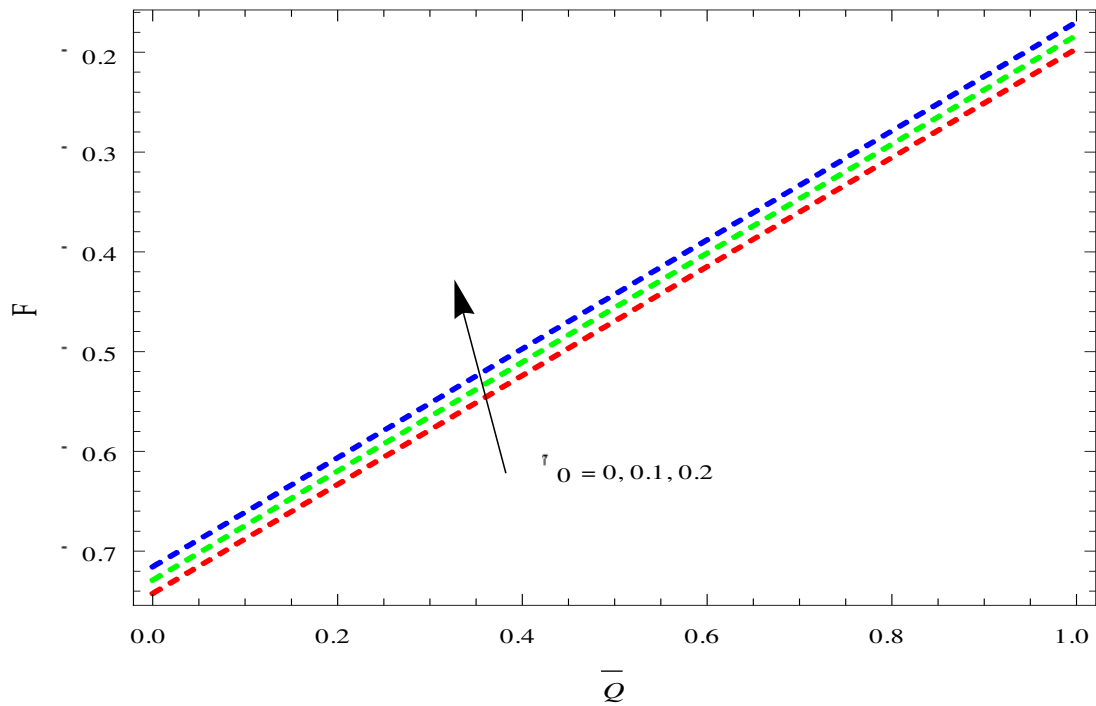


Figure 7. The deviation of F with \bar{Q} for distinct τ_0 using $\alpha = 0.7, \phi = 0.6, \mu = 0.1, \eta = 1$.

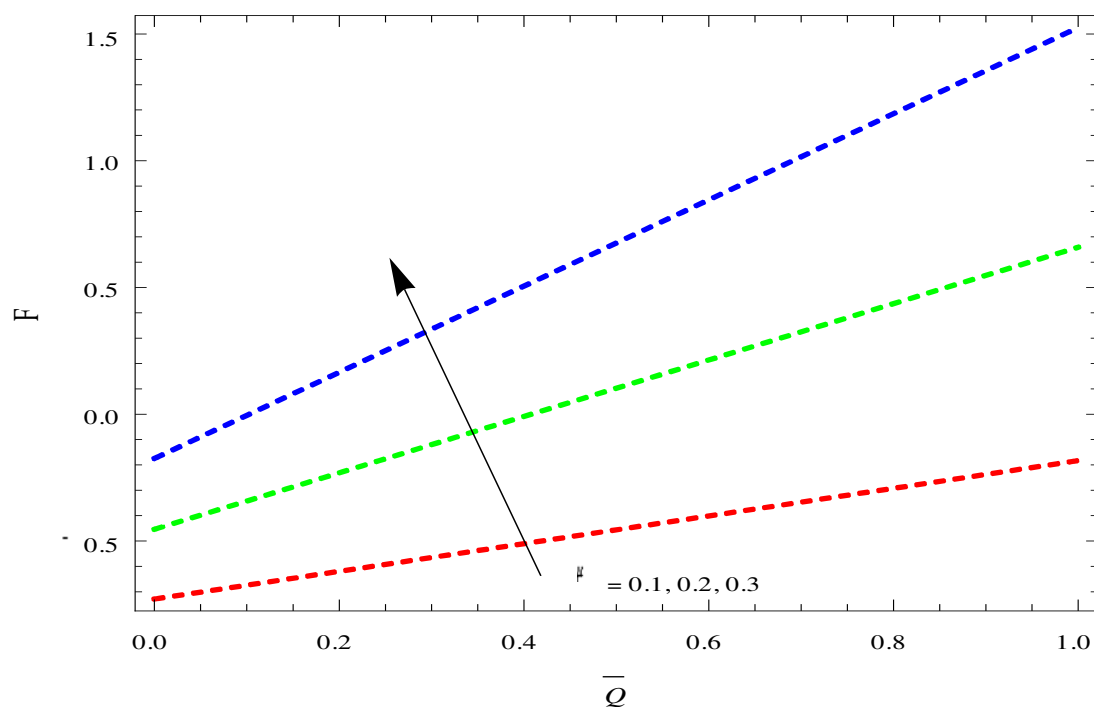


Figure 8. The deviation of F with \bar{Q} for distinct μ using $\alpha = 0.7$, $\phi = 0.6$, $\tau_0 = 0.1$, $\eta = 1$.

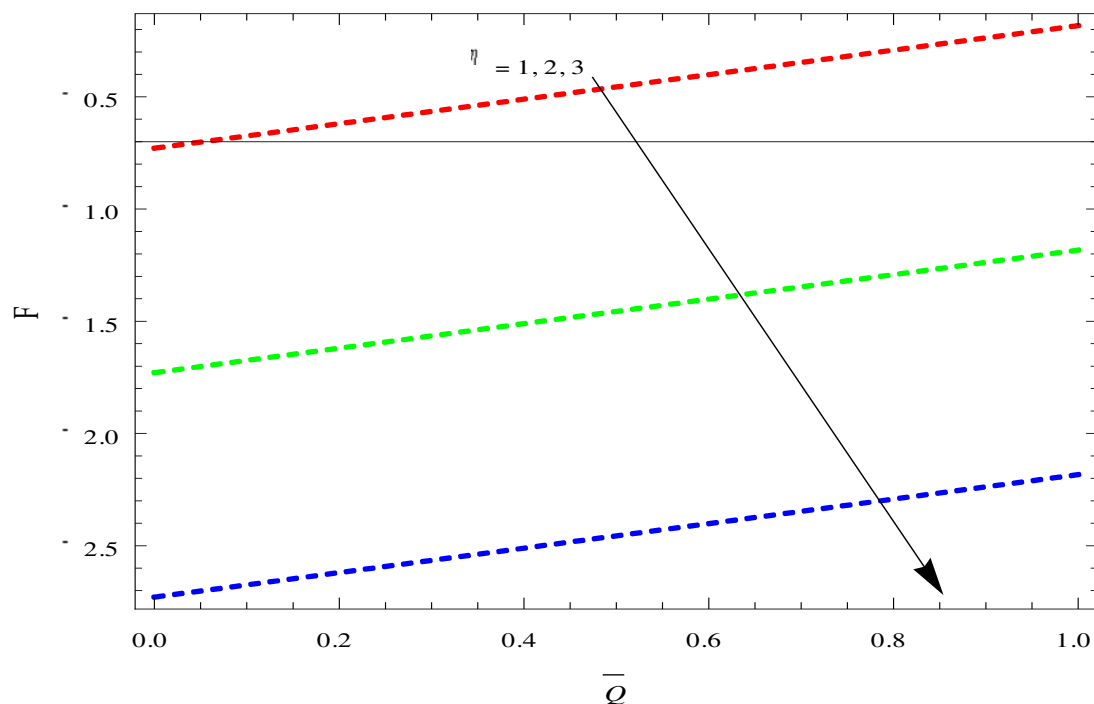


Figure 9. The deviation of F with \bar{Q} for distinct η using $\alpha = 0.7$, $\phi = 0.6$, $\mu = 0.1$, $\tau_0 = 0.1$.

References

- [1] Shapiro A H, Jaffrin M Y and Weinberg S L 1969 *J. Fluid Mech.* **37** 799-825.
- [2] Shukla J B, Parihar R S, Rao B R P and Gupta S P 1980 *J. Fluid Mech.* **97** 225-37.
- [3] Srivastava L M, Srivastava VP and Sinha SN 1983 *Biorheology* **97** 153-86.
- [4] Brasseur J G, Corrsin S and Lu N Q 1987 *J. Fluid Mech.* **174** 495-519.

- [5] Ramachandra Rao A and Usha S 1995 *J. Fluid Mech.* **298** 271-85.
- [6] Usha S and Ramachandra Rao A 1997 *ASME J. of Biomechanical Engineering*, **119(4)** 483-8.
- [7] Comparini, E and Mannucci, P. 1998 *J. Math. Anal. Appl.*, **227(2)** 359-81.
- [8] Vajravelu K, Sreenadh S and Ramesh Babu V 2006 *Quarterly of Appl. Math.* **64(4)** 593-604.
- [9] Vajravelu K, Sreenadh S, Hemadri Reddy R, Murugesan K 2009 *International Journal of Fluid Mechanics Research* **36(3)** 244-254.
- [10] Narahari M and Sreenadh S 2010 *Int. J. of Appl. Math and Mech*, **6(11)** 41-54.
- [11] Kumar M A, Sreenadh S, Saravana, R, Srinivas, A N S, Venkataramana, S 2013 *International Journal of Engineering Science and Technology (IJEST)*, **5(4)** 731-8.
- [12] Hari Prabakaran P, Hemadri Reddy R, Sreenadh S, Saravana R, Kavitha A 2013 *Adv Appl Fluid Mech*, 13(2) 127-39.
- [12] Sreenadh S, Komala, K, Srinivas, A N S 2015 *Ain Shams Eng J.*, 2015.08.019.
- [13] Kavitha A, Hemadri Reddy R, Saravana, R, Sreenadh S 2015 *Ain Shams Eng J*, <http://dx.doi.org/10.1016/j.asej.2015.10.014>.